Electronic Supplementary Material (ESI) for Green Chemistry.
This journal is © The Royal Society of Chemistry 2018

Continuous pervaporation-assisted furfural production catalyzed by $CrCl_3$

Alex Wang[a,b], Nitash P. Balsara[a,b,c*], Alexis T. Bell[a,b*]

[a] Department of Chemical and Biomolecular Engineering, University of California, Berkeley, CA 94720, USA

[b] Energy Biosciences Institute, University of California, Berkeley, CA 94704, USA

[c] Material Sciences Division and Environmental Energy Technologies Division, Lawrence Berkeley National Laboratory, Berkeley, CA 94720, USA

*To whom correspondence should be addressed: alexbell@berkeley.edu; nbalsara@berkeley.edu

Electronic Supplementary Information

Reaction rate constants of furfural production with $CrCl_3$ and H_2SO_4 at 130 °C

To determine the impact of furfural pervaporation at 130 °C, we measured the kinetics of xylose consumption and furfural formation at this temperature. These batch reactions were carried out in 10 mL thick-walled glass vials (Sigma-Aldrich, 27198) sealed with PTFE/silicone crimp top septa (Agilent, 8010-0420) and immersed in a silicone oil bath. Separate reactors were used for each reaction time. The temperature of the oil bath was maintained with a magnetic-stirring hotplate (Sigma-Aldrich, Z645060). Reactor contents were stirred using PTFE-coated stir bars rotating at a rate of 600 rpm.

For these experiments, we added 100 mM H_2SO_4 to the 25 mM $CrCl_3$, as the addition of a Brønsted acid to $CrCl_3$ has previously been found to improve both the reaction rate and the selectivity to furfural.[1] Three sets of reactions were conducted: xylose conversion without liquid-liquid extraction (LLE), xylose conversion with LLE, and furfural conversion. When xylose was converted without LLE, each reactor received 4 mL of a reactant solution comprising 250 mM xylose, 25 mM $CrCl_3$, and 100 mM H_2SO_4 in water. When xylose was converted with *in situ* LLE, each reactor received 2 mL of the same reactant solution and 4 mL of toluene. When furfural was converted, each reactor received 4 mL of a reactant solution of 125 mM furfural, 25 mM $CrCl_3$, and 100 mM H_2SO_4. Upon completion of the reaction, the reactors were removed from the oil bath and quenched in an ice bath. An aliquot of each phase (water and toluene, if applicable) was removed from the reactor for analysis by high-performance liquid chromatography (HPLC). An internal standard (5 g/L dodecane in toluene) was added to toluene-phase samples prior to analysis by gas chromatography-flame ionization detector (GC-FID). These reactions were duplicated and each resulting figure was constructed using the mean values for each time point, with the error bars representing the range of the two trials.

HPLC was conducted using an Ultra High Performance Liquid Chromatograph system (Shimadzu). 10-µL aliquots of the samples were injected onto a 300 mm × 7.8 mm Aminex HPX-87H (Bio-Rad) column equipped with a 4.6 mm × 30 mm micro-guard Cation H guard column (Bio-Rad) and a refractive index detector. The compounds were eluted at 65 °C with an isocratic flow rate of 0.4 mL/min of 0.01 N H_2SO_4 in water. Product quantities were determined by converting integrated peak areas into concentrations using a 7-point calibration curve generated from standards created with analytical grade chemicals.

GC-FID was conducted using a Varian CP-3800 Gas Chromatograph equipped with a FactorFour Capillary Column (UF-5ms 30 m, 0.25 mm, 0.25 µm, P/N CP8944) connected to a Varian quadrupole-mass spectrometer (MS) and flame ionization detector (FID). Product concentrations were determined from integrated FID peak areas using a 7-point calibration curve generated from standards created with analytical grade chemicals.

The conversion and yield for reactions starting with xylose with and without LLE are shown as a function of time in Figures S1a and S1b. The xylose isomer conversion reached 97% after 6 h, while the furfural yield reached 40-57% in the same time. Importantly, in contrast with what we found at 90 °C without H_2SO_4 (Figure 2c), *in situ* furfural extraction did affect the furfural yield, leading to a 43% increase in yield. Therefore, we expect *in situ* furfural pervaporation to have a similar effect on furfural yield.

Since the membranes used in this study were not stable at 130 °C, we examined the benefit of pervaporation at that temperature through simulations. The first step in this approach was to

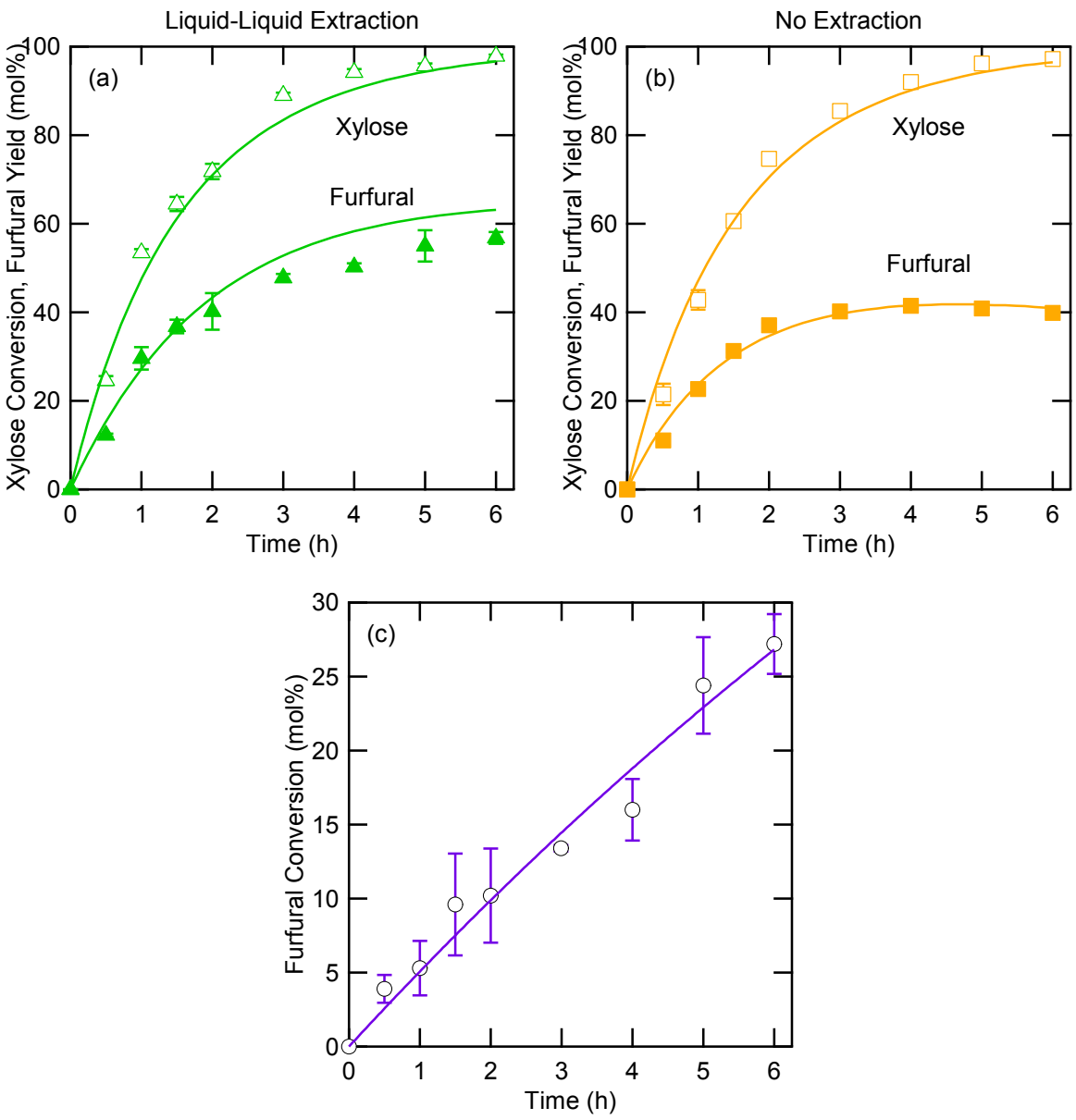

Figure S1. Batch-mode reactions at 130 °C with 25 mM $CrCl_3$ and 100 mM H_2SO_4. Data points represent experimental data, curves represent simulated results. (a) Conversion of 250 mM xylose with liquid-liquid extraction (2:1 toluene:water by volume). (b) Conversion of 250 mM xylose with no furfural extraction. (c) Conversion of 125 mM furfural.

obtain the rate coefficients governing the dehydration of xylose to furfural and the conversion of both xylose and furfural to humins. We used the reaction network shown in Scheme 1 (reproduced here as Scheme S1) to represent the kinetics of the reaction catalyzed by 25 mM $CrCl_3$ and 100 mM H_2SO_4 at 130 °C. We assumed that all reactions are first-order in xylose isomers, furfural, and intermediates, when applicable, *i.e.*

$$\frac{d[X]}{dt} = -\left(k_1 + k_4[I]\right)[X] \tag{S1}$$

$$\frac{d[I]}{dt} = k_1[X] - k_2[I] - k_3[I][F] - k_4[I][X] \tag{S2}$$

$$\frac{d[F]}{dt} = k_2[I] - k_3[I][F] - k_5[F] \tag{S3}$$

where $[X]$, $[I]$, and $[F]$ are the molar concentrations of xylose isomers, reaction intermediate, and furfural, respectively. The constants k_1, k_2, k_3, k_4, and k_5 correspond to the same constants in Scheme S1. We assumed that the intermediate exists in a pseudo-steady state, *i.e.* $d[I]/dt \approx 0$ and

$$[I] = \frac{k_1[X]}{k_2 + k_3[F] + k_4[X]} \tag{S4}$$

We measured k_5 on its own by reacting 125 mM furfural. In this case, the only relevant reaction is furfural resinification, or Reaction 5 in Scheme S1, and the expected time-dependence of $[F]$ is

$$[F] = [F]_0 \exp\left(-k_5 t\right) \tag{S5}$$

where $[F]_0$ is the initial concentration of furfural (125 mM). The comparison between experimental data and this fitting equation is shown in Figure S1c. We determined k_1-k_4 by reacting 250 mM xylose without LLE and using the value of k_5 measured previously. The comparison between the data and the simulation is shown in Figure S1b and k_1-k_5 are shown in Table 1.

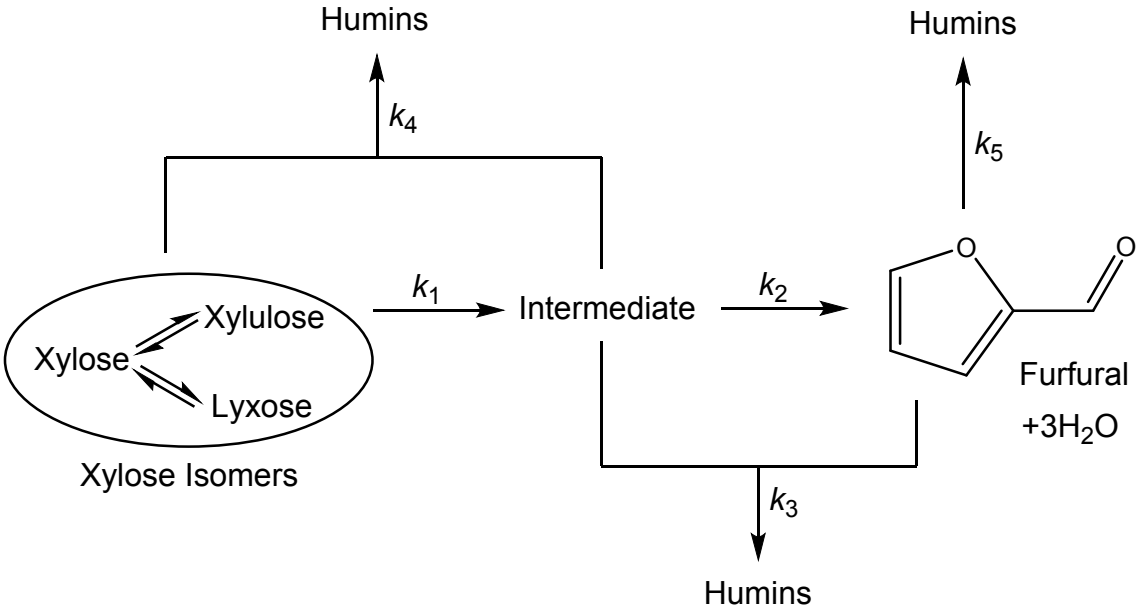

Scheme S1. Reaction network for furfural production from xylose. Isomerization is catalyzed by Lewis acids, while furfural production is catalyzed by Brønsted acids.

Next, we validated the rate constants by comparing experimental and simulated data for furfural production with furfural extraction by LLE using a 2:1 volume ratio of toluene:water. We assumed that the mass transfer rate of furfural across the two phases was very rapid, resulting in an equilibrium distribution. We measured the equilibrium distribution of furfural between water and toluene by filling 10 mL thick-walled glass vials (Sigma-Aldrich, 27198) with a PTFE-coated stir bar, 4 mL of toluene, and 2 mL of aqueous furfural solution also containing 25 mM $CrCl_3$ and 100 mM H_2SO_4. Each vial was matched to a time point from the LLE-assisted reactions with the total furfural in each vial corresponding to the total furfural produced in its matched time point. The vials were then sealed with PTFE/silicone crimp top septa, shaken vigorously by hand for 10 s, then placed on a stir plate for one hour, with the stir bar rotating at 600 rpm. The vials were then opened and an aliquot of each phase was removed for analysis, with an internal standard (5 g/L dodecane in toluene) added to toluene-phase samples prior to analysis by GC-FID. We measured this distribution to be 89.6%±1.0%, *i.e.* the toluene phase contained an average 89.6% of the furfural across the measured concentration range (the error is the standard deviation of the 16 measurements). This assumption allowed us to rewrite the furfural mole balance as follows:

$$\frac{d[F]^{aq}}{dt} = \left(\frac{1}{K\nu + 1}\right)\left(k_2[I] - k_3[I][F] - k_5[F]\right) \tag{S6}$$

$$\frac{d[F]^{org}}{dt} = \left(\frac{K}{K\nu + 1}\right)\left(k_2[I] - k_3[I][F] - k_5[F]\right) \tag{S7}$$

where $[F]^{aq}$ and $[F]^{org}$ are the concentrations of furfural in the aqueous and toluene phases, respectively, K is the equilibrium constant (*i.e.* $[F]^{org}/[F]^{aq}$, measured to be 4.31 across the

concentration range relevant to the reaction), and v is the volume ratio (*i.e.* toluene-phase volume/aqueous-phase volume = 2). The experimental and simulated data for LLE-assisted furfural production are in good agreement and are shown in Figure S1a.

Extrapolation of pervaporation data to 130 °C

We could not measure the permeability of SDS membranes at 130 °C because the membranes could not be used at that temperature. We also could not measure the activity coefficient of furfural/water solutions at our concentrations of interest at that temperature. However, we found that a simplification allowed us to combine the two parameters in order to predict the system performance for reaction with pervaporation.

The molar permeation rate of component i, $\dot{n}_i$, in pervaporation is described as follows[2, 3]:

$$\dot{n}_i = \frac{\Delta m_i}{M_i \Delta t} = A \cdot J_i = A \cdot \frac{P_i}{l}\left(x_i \gamma_i p_i^{\text{sat}} - y_i p_{\text{permeate}}\right) \tag{S8}$$

where Δm_i is the change in mass of the permeate during the length of time Δt, M_i is the molecular weight, A is the area of the membrane, J_i is the molar flux, P_i is the permeability, l is the thickness of the membrane, x_i is the mole fraction in the liquid feed, γ_i is the activity coefficient in the liquid feed, p_i^{sat} is the saturation vapor pressure at the feed conditions, y_i is the mole fraction in the vapor permeate, and p_{permeate} is the total permeate pressure.

The driving force for pervaporation is maximized by minimizing the permeate partial pressure of all components, resulting in the following simplification:

$$\dot{n}_i = A\frac{P_i}{l}\left(\gamma_i x_i p_i^{\text{sat}} - y_i p_{\text{permeate}}\right) \approx A\frac{P_i}{l}\gamma_i x_i p_i^{\text{sat}} \tag{S9}$$

Equation (S9) can then be rearranged to separate measurable quantities from those that we desire, as shown in Equation (S10):

$$\frac{\dot{n}_i l}{A x_i p_i^{\text{sat}}} \approx (P\gamma)_i \tag{S10}$$

We can measure $\dot{n}_i$, l, A, and x_i, and we can calculate p_i^{sat} by the Antoine equation,[4] allowing us to calculate the product of permeability and activity coefficient $(P\gamma)_i$.

We measured $\dot{n}_i$ at temperatures of 50-90 °C with a benchtop pervaporation unit (Sulzer Chemtech), as described in Ref [5]. A feed solution of 20 g/L furfural was used for these measurements with SDS membranes of 121-132 μm in thickness. The pervaporation experiments at 50-90 °C were conducted with two membranes per temperature, and three measurements taken per membrane. The resulting plots report the average value at each temperature, while the error bars represent the standard deviation of the six measurements.

Using Equation (S10), we determined $(P\gamma)_i$ for furfural and water for SDS membranes from 50 to 90 °C, as shown in Figure S2. We then applied an exponential fit of the data, which we could extrapolate to 130 °C to represent a hypothetical SDS membrane that could operate at that

temperature. $(P\gamma)_i$, especially for furfural, decreased as temperature increased, suggesting that the furfural flux should decrease with increasing temperature. However, since the flux is also dependent on the saturation vapor pressure, which increases dramatically with temperature as dictated by the Antoine equation, the combined result is a significant increase in the furfural flux with temperature. The saturation vapor pressures and extrapolated values of $(P\gamma)_i$ of furfural and water at 130 °C are shown in Table 1.

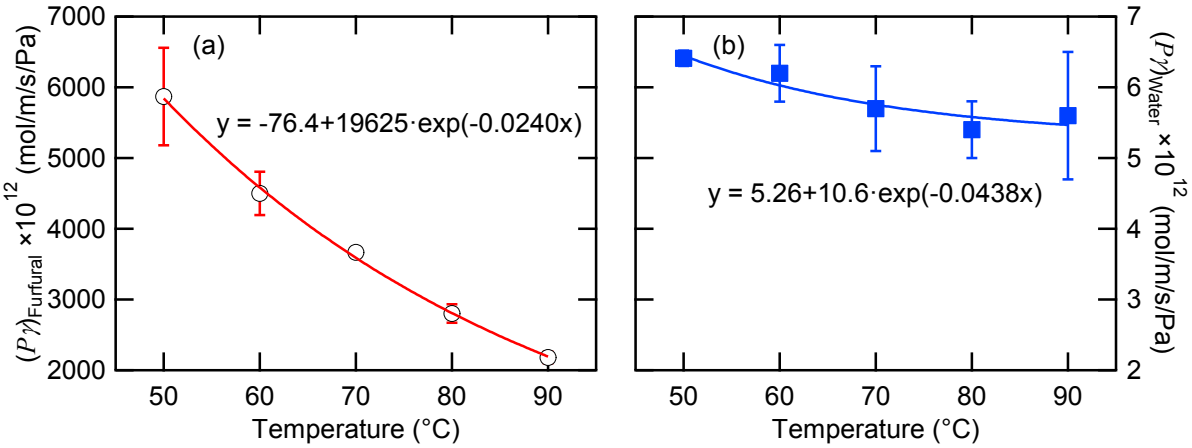

Figure S2. Change in the product of permeability and activity coefficient with temperature for SDS membranes for (a) furfural and (b) water. Equations describe the exponential fit (curves) to the data (symbols).

Simulations of pervaporation-assisted furfural production with $CrCl_3$ and H_2SO_4 at 130 °C

We then used the kinetic rate constants and extrapolated pervaporation data to predict pervaporation-assisted furfural production in water with 25 mM $CrCl_3$ and 100 mM H_2SO_4 at 130 °C. The mole balances for this approach were modified slightly.

For batch-mode reactions, a term was added to the mole balance of furfural in the reactor to represent pervaporation:

$$\frac{d[F]^{\text{ret}}}{dt} = k_2[I] - k_3[I][F] - k_5[F] - \frac{Ap_{\text{f}}^{\text{sat}}(P\gamma)_{\text{f}}}{Vl}\frac{[F]^{\text{ret}}}{[F]^{\text{ret}} + [X] + [W]} \qquad \text{(S11)}$$

where $[F]^{\text{ret}}$ is the molar concentration of furfural in the retentate (reactor), V is the reactor volume, and $[W]$ is the molar concentration of water. $[W]$ was calculated by assuming a constant solution density of 1 g/mL, such that

$$[W] = \left(1\text{g/mL} - [F]M_{\text{f}} - [X]M_{\text{x}}\right)/M_{\text{w}} \qquad \text{(S12)}$$

where M_{f}, M_{x}, and M_{w} are the molecular weights of furfural, xylose isomers, and water, respectively. In addition to the change to the furfural mole balance (Equation (S11)), we added equations describing the moles of furfural in the permeate and the volume of the permeate:

$$\frac{dN_{\mathrm{f}}^{\mathrm{perm}}}{dt} = \frac{Ap_{\mathrm{f}}^{\mathrm{sat}}(P\gamma)_{\mathrm{f}}}{l} \frac{[F]^{\mathrm{ret}}}{[F]^{\mathrm{ret}} + [X] + [W]} \tag{S13}$$

$$\frac{dV^{\mathrm{perm}}}{dt} = \frac{A}{l}\left(\frac{p_{\mathrm{f}}^{\mathrm{sat}}(P\gamma)_{\mathrm{f}}[F]^{\mathrm{ret}}M_{\mathrm{f}} + p_{\mathrm{w}}^{\mathrm{sat}}(P\gamma)_{\mathrm{w}}[W]M_{\mathrm{w}}}{[F]^{\mathrm{ret}} + [X] + [W]}\right)(1\mathrm{mL/g}) \tag{S14}$$

where $N_{\mathrm{f}}^{\mathrm{perm}}$ is the moles of furfural in the permeate and V^{perm} is the volume of the permeate. Equation (S13) matches the pervaporation term in Equation (S11), but is opposite in sign and is multiplied by V. Equation (S14) considers the permeated mass of both furfural and water and converts it to volume by assuming a solution density of 1 g/mL.

For continuous-mode reactions, we used the same differential equations as we did for the batch-mode reactions, with one more term added to the xylose isomer mole balance to describe the input of xylose:

$$\frac{d[X]}{dt} = -\left(k_1 + k_4[I]\right)[X] + \frac{[X]_{\mathrm{in}}}{V}\frac{dV^{\mathrm{perm}}}{dt} \tag{S15}$$

$[X]_{\mathrm{in}}$ is the concentration of xylose in the solution fed to the reactor. The volume of the reactor is kept constant so that the volumetric flow rate of xylose solution into the reactor matches the volumetric permeation rate.

References

1. V. Choudhary, S. I. Sandler and D. G. Vlachos, *ACS Catal.*, 2012, **2**, 2022-2028.
2. J. Wijmans and R. W. Baker, *J. Membr. Sci.*, 1995, **107**, 1-21.
3. R. W. Baker, *Membrane Technology and Applications*, John Wiley & Sons Ltd, The Atrium, Southern Gate, Chichester, West Sussex, P19 8SQ, United Kingdom, 2012.
4. J. Gmehling, U. Onken and W. Arlt, *Vapor-liquid equilibrium data collection*, DECHEMA, Frankfurt, 1978.
5. A. E. Ozcam, N. Petzetakis, S. Silverman, A. K. Jha and N. P. Balsara, *Macromolecules*, 2013, **46**, 9652-9658.